Pergamon

Int. J. Multiphase Flow Vol. 22, No. 3, pp. 613–619, 1996

0301-9322/96 $15.00 + 0.00

0301-9322(95)00084-4

BRIEF COMMUNICATION

THE EFFECT OF FLUID PROPERTIES ON TWO-PHASE (VAPOR–LIQUID) FLOW PATTERNS IN THE PRESENCE OF HELICAL WIRE RIBS

J. WEISMAN, J. LAN and P. DISIMILE
College of Engineering, University of Cincinnati, Cincinnati, OH 45221, U.S.A.

(Received 9 July 1995; in revised form 10 December 1995)

1. INTRODUCTION

Since helical ribbing is one of the widely used methods for enhancing boiling heat transfer and increasing the critical heat flux inside tubes, it is desirable to understand the flow patterns produced during vapor–liquid flow. In a previous study reported in this journal (Weisman *et al.* 1994), the air–water flow patterns produced by five different helical wire configurations were presented. The present study examines flow-pattern behavior in horizontal lines with the refrigerant 113 vapor–liquid system using two of the helical coil arrangements tested in the air–water experiments.

2. EXPERIMENTAL PROGRAM

The flow pattern studies were carried out using the University of Cincinnati's boiling freon apparatus originally described by Weisman *et al.* (1979). In this apparatus, the flow produced by a centrifugal pump proceeds through an orifice flow meter and set of vertical electrical heaters. The vapor–liquid mixture produced by the heaters flows through a 1.5 m length of horizontal 1 in. Schedule 80 pipe (i.d. 2.45 cm) and then through a 1.52 m long horizontal length of 2.54 cm i.d. glass pipe. Flow pattern observations were made at the downstream end of the test section. After proceeding through a condenser–cooler, the fluid returns to the pump.

System pressure was maintained by a nitrogen overpressure on a large diaphragm type accumulator. The synthetic rubber diaphragm prevented the nitrogen from dissolving in the refrigerant.

Vapor flow was measured by means of the signal from a specially designed drag disk. The drag disk, which was placed approximately 0.8 m downstream of the test section, consisted of a perforated disk which filled the entire tube. The disk was preceded by a fine screen since earlier tests by Weisman (1977) had shown that this configuration led to a drag disk signal which was proportional to the square of the mass velocity divided by homogenous density (density obtained taking velocity ratio = 1) of the mixture. (These results were verified just prior to the present tests.) Since the total mass flow was obtained from the orifice in the liquid stream, the drag disk signal allowed the vapor velocity to be computed.

3. FLOW PATTERN STUDIES

Flow pattern observations were obtained using a single wire coil and a double-wire coil having the dimensions shown in table 1. Both coils were previously used in the air-water tests. Tests were conducted for both configurations at 3 bar and 5 bar resulting in vapor densities which were about 11 and 18 times greater than air at room conditions. The liquid density was about 1.35 times that

Table 1. Helical rib geometries†

	Internal tube dia. (cm)	Rib height (cm)	Rib cross section	y	$P/2D$
single helix	2.54	0.32	circular	2.5	2.5
double helix	2.54	0.32	circular	2.5	1.25

†P = distance between adjacent wires; D = tube diameter; and, y = helix pitch/($2D$).

of room temperature water while the surface tension was only about 1/8 that of the air–water system. The flow pattern maps obtained with the single wire coil are shown in figure 1 while those with the double wire coil are shown in figure 2. The cross-hatched areas indicate the transition region between flow patterns. The solid lines indicate the transition lines which would have been observed with refrigerant 113 under the same conditions in a smooth tube. These smooth-tube transitions were computed using the horizontal flow pattern map of Weisman *et al.* (1979). The flow pattern designations placed next to the solid lines indicate the pattern that would be seen in a smooth tube.

With the flow pattern categorization previously used (Weisman *et al.* 1994), the overall behavior was found to be generally similar to that observed with the air-water system. Most significantly, the dispersed flow region is replaced by annular flow in which a swirling outer liquid region is clearly visible. Over a narrow range of liquid velocities just below the velocity at which true annular flow begins, the vapor bubbles did not move to the center of the tube but followed the helical path of the ribs at a short radial distance from the ribs. This flow pattern was designated as "swirl" and its transition from intermittent flow was set at the onset of swirl flow as in air–water flow. The transition to swirl and annular flow at moderate gas flows occurs at a liquid velocity substantially below the transition to dispersed flow in a smooth tube.

While the disappearance of the dispersed bubble flow pattern seen in smooth tubes at high liquid velocities may seem surprising, its absence is readily explained. At the liquid flow rates at which dispersed flow might be expected, the helical wire insert has established a strong swirling motion of the fluid. Any small bubble which might form would be rapidly moved by the centripetal force

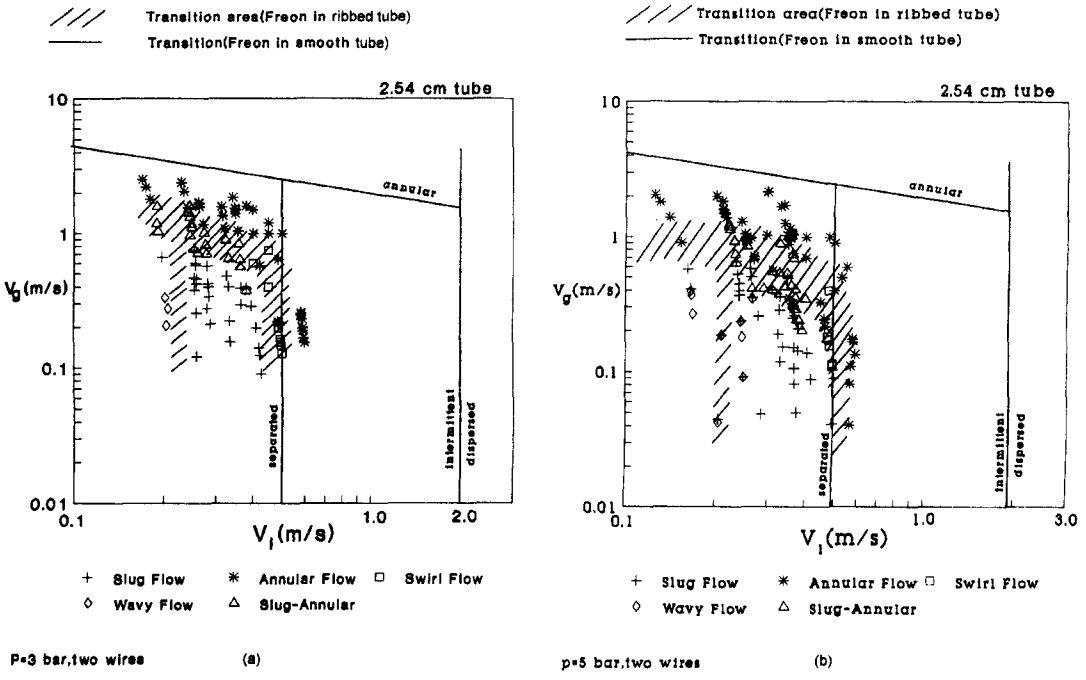

Figure 1. Flow pattern map with single helix. (a) R113 at 3 bar; (b) R113 at 5 bar.

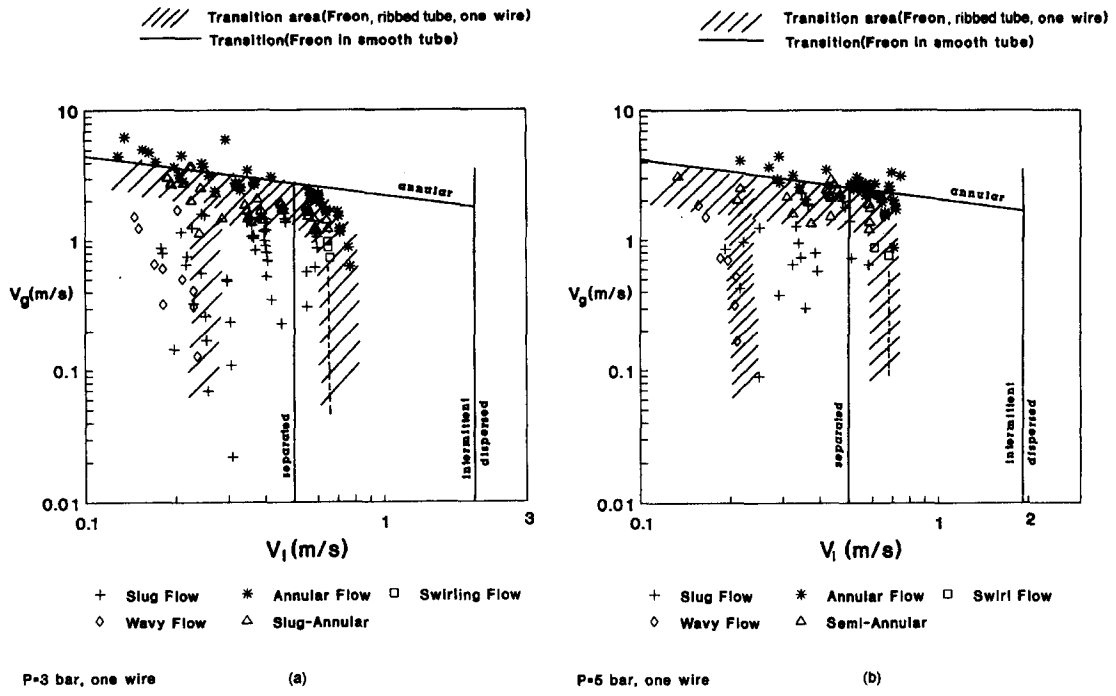

Figure 2. Flow pattern map with double helix. (a) R113 at 3 bar; (b) R113 at 5 bar.

to the center of the tube where it would join the vapor core. Dispersed bubble flow is absent in both the air–water and the refrigerant systems.

At the transition to swirl flow at low vapor flow rates with a single helical wire, the mixture density differed only slightly from that of liquid alone. A reliable estimate of the vapor flow could not be obtained at these conditions. However, the liquid velocity at which the transition occurred could be determined. The experimentally determined transition is therefore indicated as a vertical dotted line at the measured liquid flow rate. The length of the vertical line indicates the uncertainty in the gas rate.

In the single wire tests at high gas flow rates, the transition to annular flow occurred at gas flow rates only somewhat below those for a smooth tube. With the double helix the annular flow transitions were substantially below those for a smooth tube. This difference was somewhat surprising since both helical wires had the same diameter (0.32 cm). In the air–water tests, the annular flow transition at high vapor velocities depended primarily on the ratio of wire to tube diameter and was affected little by the presence of a second coil.

Another difference between the air-water and refrigerant data is the presence of a significant slug-annular region just below the transition to annular flow at high voids. Here, regions of annular flow were separated by periodic liquid slugs. In the air–water data previously observed at U.C., such behavior occurred only in a narrow transition range. The wider slug-annular range observed here is similar to that seen by Zarnett & Charles (1969) in their air–water observations in horizontal tubes containing helical wires. The flow pattern maps show the slug-annular region as part of the high-void annular flow transition area.

The intermittent-separated flow transition occurs at a nearly constant liquid velocity which is appreciably below that at which the transition occurs in a smooth tube. No swirl is observed in either the separated or intermittent region. Only slug flow was seen in the intermittent region.

4. CORRELATION OF FLOW PATTERN TRANSITIONS

Weisman *et al.* (1994) were able to describe their own and Zarnett & Charles (1969) flow-pattern transition data for air–water systems by a series of dimensionless correlations. The transition to swirl and annular flow at low and moderate void fractions occurred at a nearly constant superficial

liquid velocity for a given geometry. The superficial liquid velocity at which the transition from intermittent to annular flow occurred, V_{SL}, was given by

$$\frac{V_{SL} - V_{min}}{(gD)^{1/2}} = 0.21\left(\frac{P}{2D}\right)(d/D)^{-0.3} \quad [1]$$

where

d = wire diameter (m)
D = tube diameter (m)
g = gravitational acceleration
P = wire pitch = distance between adjacent wires
$V_{min} = 0.24$ m/s.

Since the transition to swirl and annular flow at low and moderate void fractions also occurred at a constant liquid velocity (for a given geometry) in the refrigerant 113 system, the transition velocities were compared to the air–water correlation. Both air–water and R-113 data are shown in figure 3. It may be seen that both systems are well represented by the solid line representing [1]. The onset of swirling flow at low and moderate vapor fractions would thus appear to be independent of fluid properties.

For the air–water system, the transition between separated and intermittent flow also occurred at a nearly constant superficial liquid velocity. The superficial liquid velocity for this transition was related to the onset of annular flow at low gas velocities by

$$(V_1 - V_2) = 0.24\left(\frac{P}{2D}\right)(gD)^{1/2} + 0.24 \text{ m/s} \quad [2]$$

where

V_1 = superficial liquid velocity at onset of annular flow at low qualities (m/s)
V_2 = superficial liquid velocity at separated-intermittent transition (m/s).

Upon combination with [1], the separated intermittent transition may be put in dimensionless form.

The flow maps of the previous section showed that the separated-intermittent transition for the R-113 also occurred at a constant liquid velocity for a given geometry. However, fluid properties appear to influence this transition and [2] did not represent the R-113 data. It seemed likely that

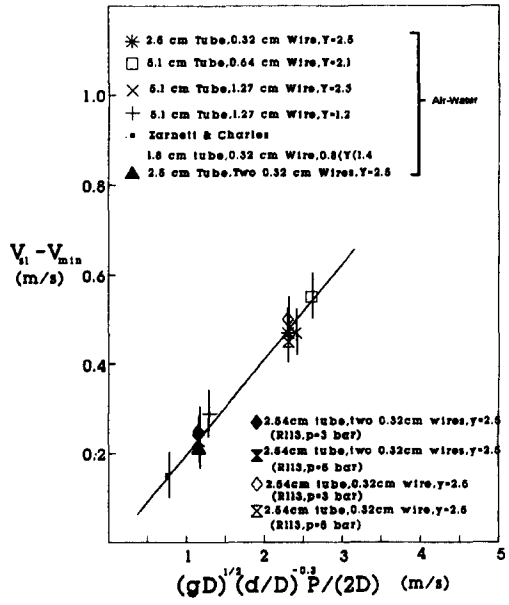

Figure 3. Correlation of annular flow transition at low void fractions.

the disappearance of intermittent flow would be influenced by the relative velocity of the vapor with respect to the liquid. By use of Lahey & Moody's (1993) suggestion, this drift velocity was represented by V_{Gj} with the flow-regime independent value given by

$$V_{Gj} = k\left[\frac{(\rho_L - \rho_G)\sigma g}{\rho_L^2}\right]^{1/4} \quad [3]$$

where

V_{Gj} = void-weighted average velocity of vapor phase with respect to the velocity of the center-of-volume of the mixture

k = constant = 2.9

ρ_G, ρ_L = vapor and liquid density, respectively

σ = surface tension.

By plotting $(V_1 - V_2)$ against $[(gD)^{1/2}(P/2D)] + V_{Gj}$ both the air-water and R-113 data may be satisfactorily represented by a single line (see figure 4)

$$(V_1 - V_2) = 0.255\left[\left(\frac{P}{2D}\right)(gD)^{1/2} + V_{Gj}\right] + 0.1. \quad [4]$$

In dimensionless form this becomes

$$(V_1 - V_2)\Big/\left[\left(\frac{P}{2D}\right)(gD)^{1/2} + V_{Gj} + 0.39\right] = 0.255. \quad [5]$$

The air–water data showed the transition to annular flow at high void fraction occurred at a vapor velocity which varied only slightly as the liquid velocity varied. This variation with liquid velocity was essentially the same as that seen in a smooth tube. The ratio of the superficial gas velocity for the annular flow transition in a smooth tube to superficial gas velocity at the transition in a ribbed tube (V_{swirl}/V_{empty}) was a constant for a given geometry. The only geometrical factor of significance was the ratio of the wire diameter to the tube diameter. The air-water data were therefore correlated by

$$(V_{swirl}/V_{empty}) = 1.1 - 2.42\ (d/D). \quad [6]$$

The values of V_{empty} were computed from the annular flow transition correlation of Weisman *et al.* (1979). The results of the computation are shown in figures 1 and 2.

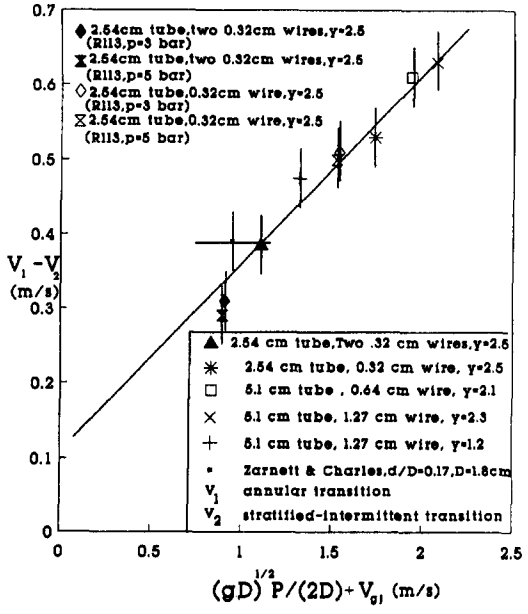

Figure 4. Correlation of separate-intermittent transition.

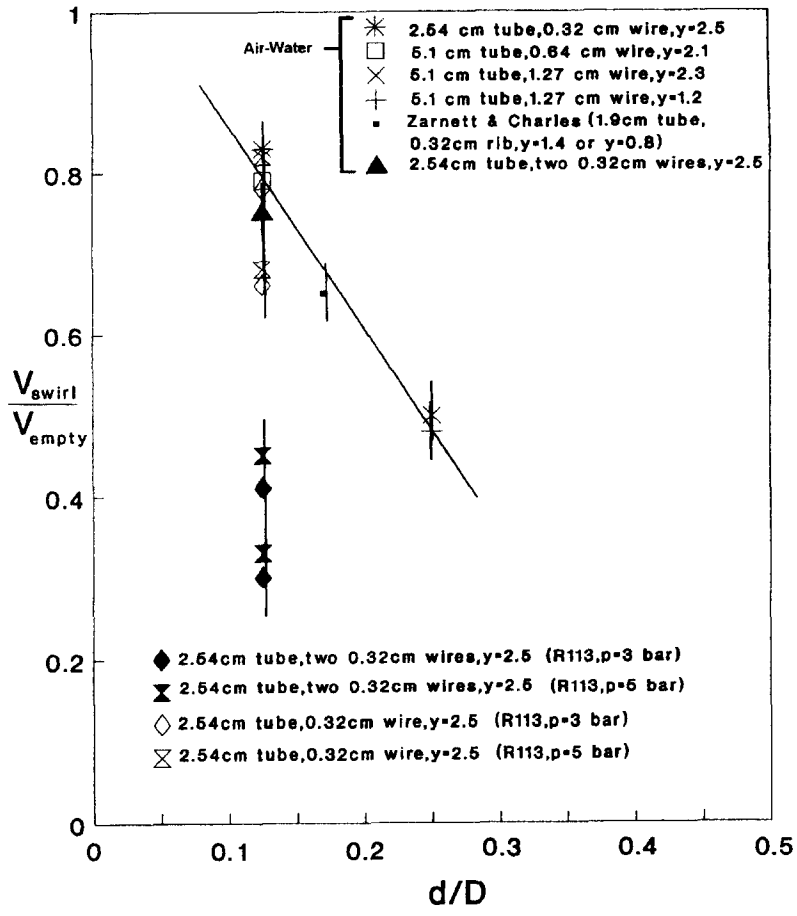

Figure 5. Annular flow transition at high void fractions.

Figure 5 treats both the R-113 and air-water data for the high void transition to annular flow in the manner which was successful for the air–water data. Because the R-113 data showed a very wide transition band, these data are represented by a double symbol connected by a vertical line. The upper symbol represents the onset of full annular flow while the lower symbol represents the onset of slug-annular flow. It may be seen that the transition to full annular flow with a single wire falls on the air–water line and the slug-annular transition is, therefore, below the line. The transition data obtained with the double helix fell significantly below the data for the single helix. The air–water data indicated little difference between the single and double helix. It would appear that effect of multiple coils depends significantly on fluid properties. However, the presently available data is insufficient to establish this relationship.

5. CONCLUSION

At low and moderate void fractions, the onset of swirling flow in horizontal lines containing helical ribs appears to be independent of fluid properties. Both air–water and R-113 data are well represented by [1]. However, fluid properties appear to influence the other transition lines. By using the vapor drift velocity, V_{gj}, to modify the separated-intermittent transition correlation developed for air–water systems, both R-113 and air–water data are represented by [5]. The previously developed correlation of the transition to annular flow at high void fractions appears to provide a reasonable representation of single helix behavior. However, a fully satisfactory correlation of double helix behavior remains to be developed.

REFERENCES

Lahey, R. T. & Moody, F. J. 1993 *The Termal-hydraulics of a Boiling Water Nuclear Reactor*, p. 248. Am. Nuclear Soc, LaGrange Park, IL.

Weisman, J. 1977 Experimental data on two-phase ΔP across area changes during transients. US Nuclear Regulatory Commission Rep. NUREG-0306.

Weisman, J., Duncan, D., Gibson, J. & Crawford, T. 1979 Effects of fluid properties and pipe diameter on two-phase flow patterns in horizontal lines. *Int. J. Multiphase Flow* **5,** 437–462.

Weisman, J., Lan, J. & Disimile, P. 1994 Two-phase (air-water) flow patterns and pressure drop in the presence of helical wire ribs. *Int. J. Multiphase Flow* **20,** 885–899.

Zarnett, G. D. & Charles, M. E. 1969 Cocurrent gas–liquid flow in horizontal tubes with internal spiral ribs. *Can. J. Chem. Engng* **47,** 238–241.